COMPUTER VISION, GRAPHICS, AND IMAGE PROCESSING 24, 363–381 (1983)

SURVEY

Digital Image Enhancement: A Survey*

DAVID C. C. WANG,† ANTHONY H. VAGNUCCI,‡ AND C. C. LI §

†*Bell Telephone Laboratories, Holmdel, New Jersey 07733;* ‡*Department of Medicine, Montefiore Hospital and the University of Pittsburgh School of Medicine, Pittsburgh, Pennsylvania 15213; and* §*Department of Electrical Engineering, University of Pittsburgh School of Engineering, Pittsburgh, Pennsylvania 15261*

Received August 24, 1981; revised March 22, 1982 and September 1, 1982

Over decades, many image-enhancement techniques have been proposed. Most of these techniques have been implemented, and their test results have been published. These techniques are surveyed, the underlying concepts briefly described, and their merits discussed. The goal is to help investigators in their selection of enhancement techniques suitable to their needs.

1. INTRODUCTION

The purpose of image enhancement is to improve picture quality. More specifically, it is employed to remove noise, to deblur objects' edges, and to highlight some specified features. Millions of pictures ranging from biomedical images to aerial photographs are generated annually [1]. The application of image enhancement, in general, improves human viewing ability and increases the chance of success in automatic picture processing [2–5]. An example is shown in Fig. 1-1 which is a computerized tomogram of a cross section of the head of a patient with a pituitary tumor (indicated by the arrow) [6]. In Fig. 1-1(b), the original picture (Fig. 1-1(a)) is degraded by additive noise such that the tumor is not visible. After the application of a smoothing scheme, the tumor becomes again clear as shown in Figs. 1-1(c) and (d).

Over decades, many image-enhancement techniques have been proposed. Most of these techniques have been implemented, and their test results have been published. In this paper, we survey these techniques, briefly describe the underlying concepts, and discuss their merits. The goal of this survey is to help investigators in their selection of enhancement techniques suitable to their needs.

Image restoration is considered as image enhancement by some authors; it is not, however, included in this paper. Image restoration attempts to estimate the "true" image of an observed picture given, if possible, a priori knowledge of the degradation [7]. Its emphasis is on degradation modeling and on image recovery by inversion of the degrading process [8]. Its goal is to obtain a picture with "enhanced" objects which differ as little as possible from those in the "true" image. Optimization of some prespecified objective criteria is thus required. On the other hand, image enhancement, to be discussed in this paper, is designed to manipulate the image on

*Supported in part by a grant from the Western Pennsylvania Heart Association. Work done while D. C. C. Wang was with the University of Pittsburgh School of Medicine.

0734-189X/83 $3.00

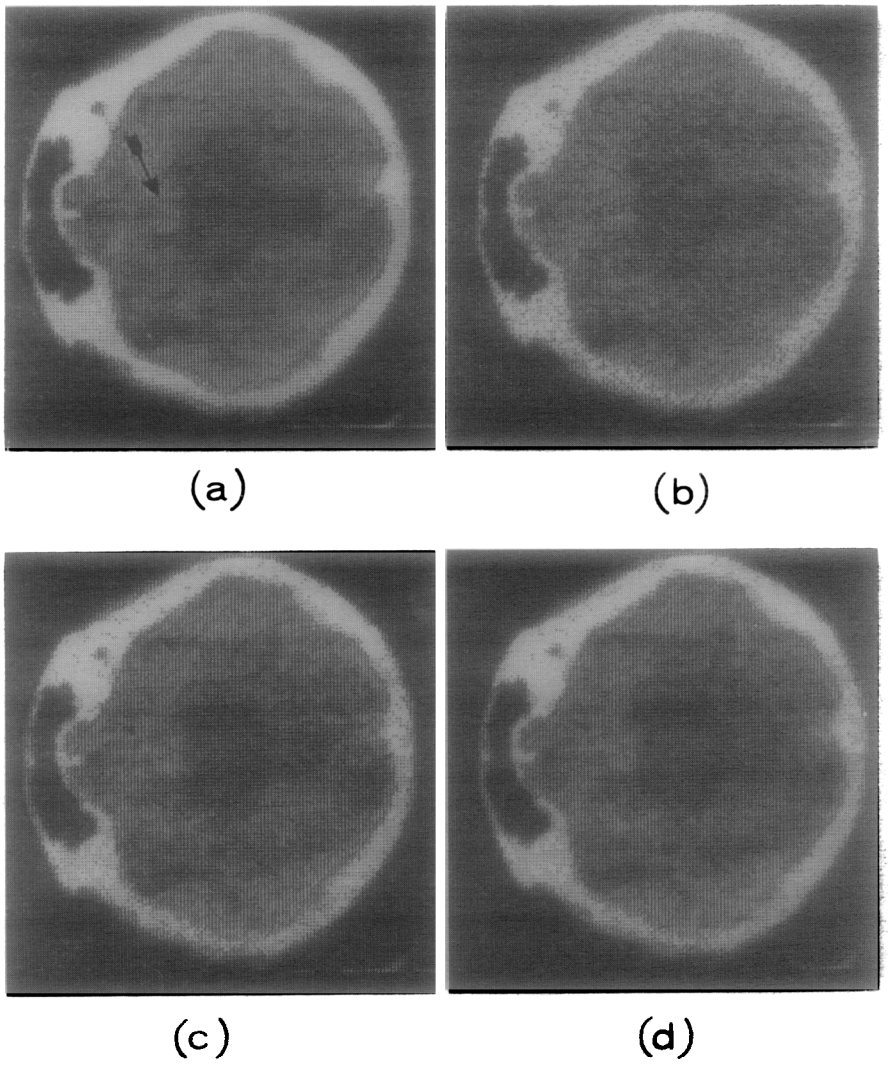

FIG. 1-1. (a) CT scan of a cross section of the head of a patient with a pituitary tumor (indicated by arrow). (b) Image degraded by additive noise. (c) and (d) The degraded image smoothed three and five times, respectively. See Wang *et al.* [6]. Reproduced by permission of the publisher.

the basis of the psychophysical characteristics of the human visual system [8]. It may even "distort" the image by deemphasis of irrelevant materials and enhancement of features of interest [9, 10].

Most of the existing image-enhancement techniques are heuristic and problem oriented [11]. Each technique is devised to handle some special kind of pictures. Modeling of the degradation process, in general, is not required; however, knowledge of the degradation phenomena may give a guide to investigators in their choice of enhancement techniques. For monochromatic images, the degradation may be categorized into point degradation, spatial degradation, and their combination. Point degradations, which include additive and multiplicative noise, do not blur the

image, but distort the gray levels of pixels. These degradations might be due to film grain, lens shading, scatter light, and other optical sensor defects. Spatial degradations, on the other hand, smear the image so that it loses resolution, and the transition from object to background becomes unclear. These degradations might be due to diffraction, optical system aberrations, defocusing, object motion, etc. For a more detailed discussion of sources of degradations, the reader is referred to some review articles and books [12–17].

Since most of the image-enhancement techniques are problem oriented, the success of the application of a technique to a particular image depends on the subjective judgment of the viewer [11]. No universal quantitative evaluation criterion is available currently. Readers are advised to apply several appropriate techniques to their images, and to choose the best one, based on their own judgment, for that image which best fits their purpose. In this paper, the enhancement techniques are evaluated on the basis of their practical applicability and computational complexity. Because computation facilities vary, some techniques may be considered too complex by some investigators, not so by others.

In Section 2, we define the notation used in this paper. In Section 3, we outline a classification of the existing techniques according to their properties. We then survey these techniques, according to the suggested classification, in Sections 4 to 7.

2. NOTATION

The notation used in this paper is listed below:

$g(x, y)$	Gray level of the pixel at coordinates (x, y) of the observed image;
$g'(x, y)$	Gray level of the pixel at (x, y) of the enhanced image;
$\mathbf{W}$	A 3×3 weighting-factor matrix for smoothing where each element is a weighting factor;
$P(g(x, y))$	Value of cumulative distribution function of an observed image at gray level $g(x, y)$;
$\nabla^2 g(x, y)$	Laplacian of the observed image at (x, y);
$g_{\max}$	Maximum gray level of the observed image;
$g_{\min}$	Minimum gray level of the observed image;
$G(f_x, f_y)$	Fourier-transformed image of the observed image;
$G'(f_x, f_y)$	Fourier-transformed image of the enhanced image;
$H(f_x, f_y)$	Frequency domain filtering function.

3. CLASSIFICATION OF ENHANCEMENT TECHNIQUES

Image enhancement is achieved by image processing through operators. The existing techniques can be categorized on the basis of the properties of their operators. Classifications are based on (1) the operator's sensitivity to image context, (2) the area which the operation covers, (3) the goals of the operation, and (4) the technical methods involved.

According to the operator's sensitivity to image context, enhancement techniques can be classified as (a) context-free, and (b) context-sensitive [4]. A *context-free*

technique provides a position-invariant operator in which all the parameters are fixed a priori. A *context-sensitive* technique furnishes a position-variant operator in which the parameters change in response to local image characteristics. A context-free operator is computationally simpler to apply. However, for pictures with variable information content, a context-sensitive operator is more suitable.

In accordance with the area covered by the operator, the existing techniques can be divided into local and global. *Local operators* take a subimage into consideration at each time; they can be further subdivided into fixed-sized and variable-sized. In a *global operation*, the whole image is involved. Computationally, application of a local operator requires less storage than that of a global operator.

Based on their goals, the existing techniques can be grouped into (a) noise cleaning, (b) feature enhancement, and (c) noise cleaning plus feature enhancement. It is well known that a picture can be degraded by additive noise, and be smeared by point-spread functions. *The noise-cleaning operator* aims at the removal of random noise; in other words, it disregards irrelevant information. The *feature-enhancement operator* attempts to decrease the blurring, and to reveal the features of interest. These two operators deal with different degradation phenomena; in practice, however, many operators are a combination of both.

According to the technical methods involved, the published techniques can be organized into four groups. They are

(a) *Spatial smoothing* of regions, which employs linear or nonlinear spatial-domain low-pass filters;

(b) *Gray-level rescaling*, which manipulates or requantizes gray levels for contrast enhancement;

(c) *Edge-enhancement*, which involves linear or nonlinear spatial-domain high-pass filters;

(d) *Frequency-domain filtering*, which utilizes low- or high-pass filters in the frequency domain where Fourier transformation is required.

The last classification is more comprehensive than the other three listed above. It specifies the technical tools which implicitly indicate the goal of the technique. In the following sections, we shall survey the existing techniques according to this classification.

4. SPATIAL SMOOTHING OF REGIONS

In this section, the observed image is assumed to be the true image degraded by random noise. Although it may not be explicitly stated, most authors who employ spatial smoothing implicitly assume that the random noise is additive and normally distributed with zero mean. Thus, smoothing, linear or nonlinear, over a region tends to remove the noise at each pixel.

The techniques described in this section provide local operators, unless otherwise stated. The required storage is usually small. The goal is noise cleaning. Some of the techniques even smear the observed image. Thus, edge enhancement may be needed afterward.

The simplest smoothing technique is equal-weighted averaging over a neighborhood [9, 10, 18, 19]. It can be expressed as follows:

$$g'(x, y) = \sum_{i=-m}^{m} \sum_{j=-n}^{n} w(i, j) \quad g(x - i, y - j) \tag{4-1}$$

where the weighting factors $w(i, j)$ are equal and

$$w(i, j) = \frac{1}{(2m + 1)(2n + 1)}. \tag{4-2}$$

In (4-1), the gray level at (x, y) is replaced by the gray level average over a $(2m + 1)$ by $(2n + 1)$ rectangular neighborhood surrounding (x, y). This simple smoothing scheme can remove noise efficiently; it will, however, blur the picture, especially at the edges of objects. Blurring becomes more severe as m and n increase.

To reduce the blurring effect, several unequal-weighted smoothing techniques have been introduced. These techniques weight the gray level at (x, y) more than those of its neighbors. Graham [20] used a 3×3 neighborhood, and the weighting factor matrix

$$\mathbf{W} = \begin{bmatrix} 0.25 & 0.5 & 0.25 \\ 0.5 & 1 & 0.5 \\ 0.25 & 0.5 & 0.25 \end{bmatrix} \tag{4-3}$$

Brown [21] proposed the weighting factor matrix

$$\mathbf{W} = \begin{bmatrix} 1 & 1 & 1 \\ 1 & 2 & 1 \\ 1 & 1 & 1 \end{bmatrix}. \tag{4-4}$$

In formulas (4-2) to (4-4), the weighting-factor matrices are context-free. They are easy to implement. However, (4-2) tends to smear the sharpness of the edge severely. Procedures (4-3) and (4-4) may not remove the noise as efficiently as (4-2); they do blur the edge, although not to the same extent as (4-2).

To improve the results obtained by the above schemes, Lev *et al.* [22] proposed a context-sensitive weighting-factor matrix. Let $g(x, y) = e$, and the gray levels of its neighbors be

$$\begin{matrix} a & b & c \\ d & e & f \\ g & h & i \end{matrix}$$

The proposed weighting-factor matrix is

$$\mathbf{W} = \tfrac{1}{9} \begin{bmatrix} \alpha\gamma\varepsilon & \alpha\gamma\eta & \alpha\xi\eta \\ \alpha\varepsilon\theta & 1 & \delta\xi\eta \\ \beta\varepsilon\theta & \beta\delta\theta & \beta\delta\xi \end{bmatrix} \tag{4-5}$$

where

$$\alpha = \exp(-|(a+b+c)-(d+e+f)|/\sigma),$$
$$\beta = \exp(-|(g+h+i)-(d+e+f)|/\sigma),$$
$$\gamma = \exp(-|(a+b+d)-(c+e+g)|/\sigma),$$
$$\text{etc.}$$

and σ is a prespecified parameter. In (4-5), the weighting is reduced in the direction which shows a sharp change in the gray level. The homogeneous area is weighted more. The blurring effect at the edge can be decreased. This technique does yield better results. Computationally, it is more complicated than the previous three. It also requires the specification of σ, which may need a priori knowledge or some trials to obtain the best result.

According to criteria similar to those suggested by Lev *et al.* [22], Wang *et al.* [6] proposed a computationally simpler 3×3 weighting-factor matrix. The matrix is

$$\mathbf{W} = \begin{bmatrix} w(x-1, y-1) & w(x-1, y) & w(x-1, y+1) \\ w(x, y-1) & w(x, y) & w(x, y+1) \\ w(x+1, y-1) & w(x+1, y) & w(x+1, y+1) \end{bmatrix} \tag{4-6}$$

where

$$w(x+k, y+l) = \tfrac{1}{2}\left[\sum_k \sum_l \delta(x, y; k, l)\right]^{-1} \delta(x, y; k, l) \qquad l, k = -1, 0, 1$$
$$w(x, y) = \tfrac{1}{2}$$

and

$$\delta(x, y; k, l) = 1/|g(x+k, y+l) - g(x, y)|$$

This technique smoothes images with very little blurring effect. It requires no prespecified parameters. However, it may not remove the noise as rapidly as the first three techniques presented above.

Graham [12] defined two measures of flexure Δ_x and Δ_y, which are approximations to the second-order derivatives of pixel gray level in the x and y directions, respectively. He then replaced $g(x, y)$ by $g'(x, y)$ where

$$g'(x, y) = \begin{cases} \frac{1}{9} \sum_{i=-1}^{1} \sum_{j=-1}^{1} g(x-i, y-j), & \text{if } \Delta_x \le T \text{ and } \Delta_y \le T \\ \frac{1}{3} \sum_{j=-1}^{1} g(x, y-j), & \text{if } \Delta_x > T \text{ and } \Delta_y \le T \\ \frac{1}{3} \sum_{i=-1}^{1} g(x-i, y), & \text{if } \Delta_x \le T \text{ and } \Delta_y \ge T \\ g(x, y), & \text{if } \Delta_x \ge T \text{ and } \Delta_y > T \end{cases} \tag{4-7}$$

and T is a prespecified threshold parameter. This scheme smooths only the homoge-

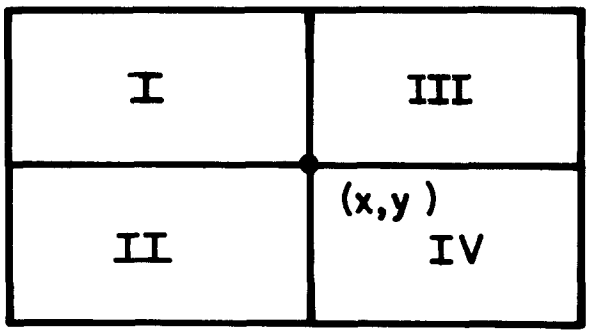

FIG. 4-1. Four neighboring regions used by Kuwahara *et al.* [23].

neous area, that is, the area with a small second derivative. It does not smooth the edge pixels. However, it ignores those isolated noise pixels which are much darker or brighter than their neighbors. In addition, this technique depends on the specification of the parameter T which requires a priori knowledge or some trials.

Another smoothing scheme suitable to clean up "pepper and salt" noise, that is, isolated noise, has been suggested [9, 15, 18, 20]. In this scheme, the gray levels of those pixels which are much darker or much brighter than their neighbors' average are replaced by the average gray level. Thus, only isolated dark points in a light region and isolated light points in a dark region are smoothed. This scheme also requires the specification of the threshold.

Kuwahara *et al.* [23] and Tomita *et al.* [24] proposed a smoothing scheme which replaces the gray level at (x, y) by the average gray level of its most homogeneous neighboring region. Kuwahara *et al.* [23] divided the neighborhood into four regions as shown in Fig. (4-1), and Tomita *et al.* [24] partitioned it into five regions, as illustrated in Fig. (4-2). They then calculated the average and variance of gray levels within each region. The region which has the smallest variance is considered as the region which does not include boundaries. The gray level at (x, y) is then replaced by the average of this region. This technique can achieve both noise removal and edge enhancement since the smoothing operation does preserve the image's edges. This scheme does not, however, yield good results when applied to images with

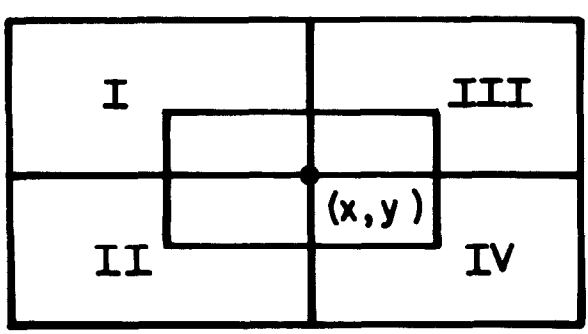

FIG. 4-2. Five neighboring regions employed by Tomita *et al.* [24].

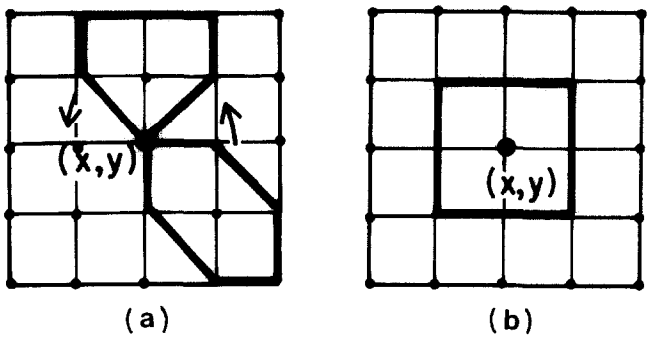

FIG. 4-3. (a) Four pentagonal and four hexagonal regions. (b) A square region used in [25].

complex-shaped regions because it employs four or more large rectangular areas as neighborhood regions.

A revision and improvement of the last two techniques was published by Nagao and Matsuyama [25]. These authors divide the 5×5 neighborhood of (x, y) into nine regions as shown in Fig. (4-3). The nine regions are four pentagonal and hexagonal regions (Fig. 4-3(a)), and a 3×3 square region (Fig. 4-3(b)). By the same criteria used in the previous techniques [23, 24], $g(x, y)$ is replaced by the average of the region which has the smallest variance. This smoothing scheme is iterative; the iteration stops when no change of the gray level occurs. The results thus obtained present a significant improvement over those derived from the previously mentioned techniques [23, 24]. However, the computation of this scheme is far more complex and time consuming; also it may smooth out the fine features of the image.

Anderson and Netravali [26] suggested a weighted smoothing procedure based on subjective criteria. The weighting factors are found by optimizing an objective function which maximizes noise suppression and minimizes blurring. This scheme has been simplified by Trussell [27]. Since human eyes can tolerate more noise in areas of high signal strength, Trussell's scheme leaves the image alone in areas of high activity, and smooths the noisy image in areas of low activity. Let the difference between the observed image $g(x, y)$ and the blurred (smoothed) image $b(x, y)$ be D. If the smoothed image $b(x, y)$ perfectly fits the "true" picture, then $\sigma_D^2 = \sigma_n^2$. In other words, the variance of D equals the variance of the noise. If $\sigma_D^2 \leq \sigma_n^2$, the smoothed image is an adequate representation of the "true" image. Otherwise, it is not adequate. Trussell interactively selects a low activity area, and calculates the variance of that area and lets the variance be σ_n^2. For each pixel (x, y) and its neighbors, he calculates $\sigma_D^2(x, y)$. Then $g(x, y)$ will be replaced by

$$g'(x, y) = \theta(x, y)b(x, y) + (1 - \theta(x - y))g(x, y) \tag{4-8}$$

where

$$\theta(x, y) = \min\{1.0, \sigma_n^2/\sigma_D^2(x, y)\}.$$

Those areas which have higher activities, i.e., large σ_D^2, show less deviation from the observed image. This technique is suitable for many images; however, its effectiveness is weakened if the noise is not uniformly distributed across the whole image.

A nonlinear smoothing scheme, called median filtering, was first proposed by Tukey [28], and then adapted by others [15, 29–32]. The filtering operation replaces $g(x, y)$ by the median gray level of a $(2m + 1)$ by $(2n + 1)$ neighborhood surrounding (x, y). This smoothing technique performs satisfactorily in step functions and ramp functions. However, the pulse functions whose periods are less than n (i.e., one-half the window width) are suppressed. Thus, in some cases, the median filter provides noise removal, and in other cases, it may cause signal suppression. To remedy this, Pratt [15] suggests using variable window widths. He starts the filtering operation by letting $n = 1$, and repeats the operation by increasing n. The process is terminated when the filtering begins to do more harm than good. This revised median filtering may improve the result; however, it is time consuming, and different n's for different regions in one image may be needed.

To avoid the noise introduced during the digitization of the picture, averaging over multiple digitized copies has been suggested [9, 18, 33]. The arithmetic mean of each pixel over the copies is employed to eliminate additive noise which is due to light scattering, electronic scattering, etc. The geometric mean is utilized to clean multiplicative noise which is due to the randomness of film grain formation, lens defects, etc.

5. GRAY LEVEL RESCALING

Gray level rescaling directly requantizes or maps each pixel to a new gray level to improve the contrast of a picture. Image-enhancement techniques which utilize gray level rescaling are different from those techniques presented in the last section. In general, gray level rescaling takes into consideration one pixel at a time, and is independent of its neighbors. The goal is object enhancement, and most of the operations are global.

In many pictures, the gray levels of the objects are so close to that of the background that it is difficult to discriminate them. Contrast enhancement is thus needed to increase the gray level differences between objects and background. In other situations, the gray levels of a large percentage of pixels concentrate in a narrow portion of the histogram. This makes the fine details hardly visible. Requantization or rescaling to increase dynamic range and to single out hidden fine structures is thus required.

The simplest technique of this category is a functional mapping of the gray level $g(x, y)$ [3, 9, 12, 34–36], i.e.,

$$g'(x, y) = f(g(x, y)) \tag{5-1}$$

where $f(\cdot)$ is a prespecified function. Some of the most popular mapping functions are illustrated in Fig. 5-1. Figures 5-1a to d are piecewise linear functions, and Fig. 5-1e is nonlinear. In Fig. 5-1a, the dark area is stretched, and the bright area is compressed. Thus, the contrast in the dark area is increased. In 5-1b, the operator performs opposite to that of 5-1a, and in 5-1c it stretches the midrange gray levels. The operator of Fig. 5-1d carries out a level slicing in which the two most significant bits are removed. Figure 5-1e shows two gamma curve corrections for film and display nonlinearities. These mappings are very easy to implement, and usually yield satisfying results. However, trial and error is needed to obtain the best results. In many cases, the investigator has to provide his own mapping functions.

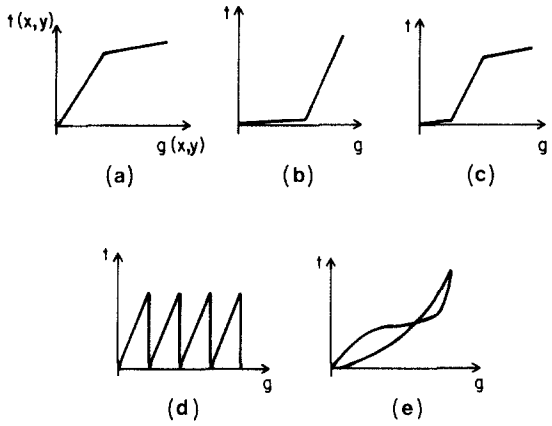

FIG. 5-1. Gray level rescaling functions: (a) dark area stretched; (b) light area stretched; (c) midrange stretched; (d) level slicing; (e) gamma function.

The gray level histograms of most images, in general, show bright or dark peaks. Figure 5-2a exhibits a histogram skewed toward dark gray levels; the peak represents a large dark area which may contain some information with fine details. To enhance this information, a technique called histogram linearization has been proposed and adopted [15, 37–43]. This technique tends to map the observed gray levels into new gray levels such that the new picture has a uniform gray level histogram. The operation is equivalent to maximizing the zeroth-order entropy. It has been suggested [44] that the information in the observed image is thus maximized for the observer; in the new picture, the dynamic range of the dark area will be expanded. Curve 1 of Fig. 5-2b is the cumulative distribution function (CDF) of a picture with

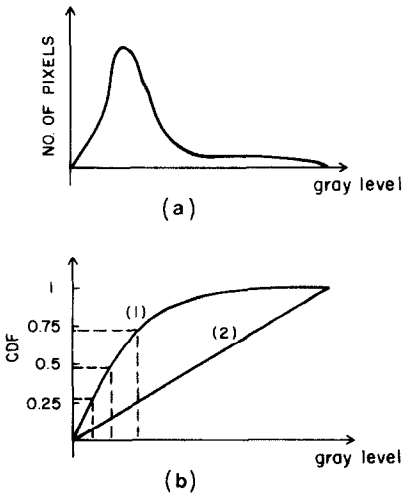

FIG. 5-2. (a) Gray level histogram of a typical image. (b) Curve 1 is the cumulative distribution function (CDF) of (a). Curve 2 is the desired linear CDF. See text.

continuous gray levels. Curve 2 is the desired linear CDF. The procedure to linearize the observed CDF (curve 1) consists of the following steps: (a) selection of equal intervals in the ordinates as shown in Fig. 5-2b; (b) from curve 1, map the intervals in the ordinate to the gray levels in the abscissa; (c) requantize the observed picture. This procedure can be formulated as [15]

$$g'(x, y) = [g_{\max} - g_{\min}]P(g(x, y)) + g_{\min} \tag{5-2}$$

where $P(g(x, y))$ is the CDF, and $g_{\max}$, $g_{\min}$ are the maximum and minimum gray levels in the observed image, respectively.

In the above procedure, an exact linearization is a practical impossibility because the gray levels are discrete; an approximate linearization of the CDF would yield a smaller number of gray levels in the enhanced image. This would create a larger quantization error [15]. A technique which performs histogram linearization with the same number of gray levels for the observed and for the enhanced images is required.

Suppose that there are n pixels in the observed image with gray level l (i.e., bin l in the histogram). Suppose also that in order to create a uniform histogram without reduction of the gray level numbers, this bin has to be broken up such that n' pixels are assigned to gray level l', and the remaining pixels to level $l' + 1$. A simple way to do so is to choose these n' pixels randomly from the n pixels. To avoid randomness in the selection of the pixels, a procedure called GRATRN has been proposed [38]. In this procedure, the average gray level s of the neighborhood around each of these n pixels is calculated. A CDF of these n average gray levels is constructed. Select, then, an average gray level s', such that the number of pixels with $s \leq s'$ equals n'. These n' pixels are then assigned to a new gray level l'. The remaining pixels with $s \geq s'$ are assigned to $l' + 1$. GRATN breaks each bin according to the average of the neighboring pixels of each pixel in that bin; the breaking, however, is somehow arbitrary, particularly for those pixels at the edge. This technique is time consuming, especially in those cases where the number of bins is very large.

It has been pointed out that human perception performs a nonlinear transformation of the light intensity [44–47]. To include human perception in the image enhancement, histogram hyperbolization [15, 44] is preferred to histogram linearization. The desired histogram of the computer enhanced image is thus of the hyperbolic form. The transforms are as follows [15]:

$$\begin{aligned}
g'(x, y) &= g_{\min} + \frac{1}{\alpha}\ln[1 - P(g(x, y))] \quad \text{for exponential histogram} \\
g'(x, y) &= \left[\left(g_{\max}^{1/3} - g_{\min}^{1/3}\right)P(g(x, y)) + g_{\min}^{1/3}\right]^3 \quad \text{for cubic root output histogram} \\
g'(x, y) &= g_{\min}\left[\frac{g_{\max}}{g_{\min}}\right]^{P(g(x, y))} \quad \text{for logarithmic output histogram}
\end{aligned} \tag{5-3}$$

where α is a constant. According to the perception performed by the rods and cones of the human retina, the perceived image would have a uniform histogram.

A scheme called iterative histogram thinning, which achieves results opposite to those obtained by histogram linearization, is proposed to thin each peak in the histogram [48, 49]. Let the number of pixels in bin i of the histogram be B_i. This scheme examines each bin i and its neighboring 2γ bins on two sides. If B_i is greater than the average A of $B_{i+1},\ldots,B_{i+j}$, a ratio $\beta = (B_i - A)/B_i$ is computed. Then the gray levels of $B_{i+j}\beta$ pixels are changed from $i + j$ to $i + j - 1, j = 1, 2, \ldots, \gamma$. Thus, B_i increases and its neighboring bins decrease. This technique yields images with homogeneous objects and background with enhanced contrast; it may, however, result in quantization error.

A noise-cheating image-enhancement scheme has been proposed [50, 51] to suppress noise and to enhance contrast. A 4×4 average (not moving average) over the observed image is performed, and followed by a 2×2 average. A 512×512 image is thus reduced to 64×64. The averaged image is then requantized such that the difference between two consecutive gray levels is at least four standard deviations. In the requantized image, isolated points are deleted. The 4×4 averaged image is then quantized. Each pixel in the 4×4 averaged image is assigned a value chosen from its surrounding points in the quantized 8×8 averaged image. The value is chosen such that the difference between before and after quantization is a minimum. Good results have been obtained by this technique; it is, however, a complex procedure, and extremely small objects may be lost in the averaging step.

Image subtraction is commonly used in serial angiography [52–55] to deemphasize the irrelevant material and to enhance the material of interest. The original radiograph is subtracted from the subsequent image. The subsequent image is obtained in the same way as the original, except that a radio-opaque substance is injected into an artery of the patient. Thus, the blood vessels are enhanced while bony structures are unchanged. Hence, image subtraction can eliminate bones, and enhance the blood vessels. The earlier work was done optically. Hall, *et al.* [39] discussed image subtraction by digital procedure. Recent developments are reviewed in [78].

6. EDGE ENHANCEMENT

In edge enhancement, we attempt to deblur the edge of an object within an image. In other words, the technique is employed to increase the gray level difference between the edge pixels of the object and of its neighboring background. Most of the edge-enhancement operators are context-free and local.

Effects which blur pictures are diffusion, defocusing, and object motion. The gray level profile at an "ideal" edge is a step function. Diffusion and defocusing blur the edge into a ramp function. The gray level at the edge of an object is decreased, and that at its neighboring background is increased. The contrast at the edge is thus reduced or even lost. To eliminate these blurring effects, an antidiffusion operator has been proposed and adopted [9, 15, 56–61]. To eliminate the effect of object motion, image restoration can be applied [14].

An anti-diffusion operation makes up for the loss of gray level at the object edge and subtracts the increment of gray level at its neighboring background. Figures 6-1a and b show a perfect one-dimensional step function $u(x)$ and its second-order derivative $\nabla^2 u(x)$, respectively. By subtracting $\nabla^2 u(x)$ from $u(x)$, we obtain the graph illustrated in Fig. 6-1c. It can be seen that the gray level difference between the edge ($x = 0^+$) and its neighboring background ($x = 0^-$) is increased. The overshooting of gray levels at the edge will enhance the edge. The anti-diffusion

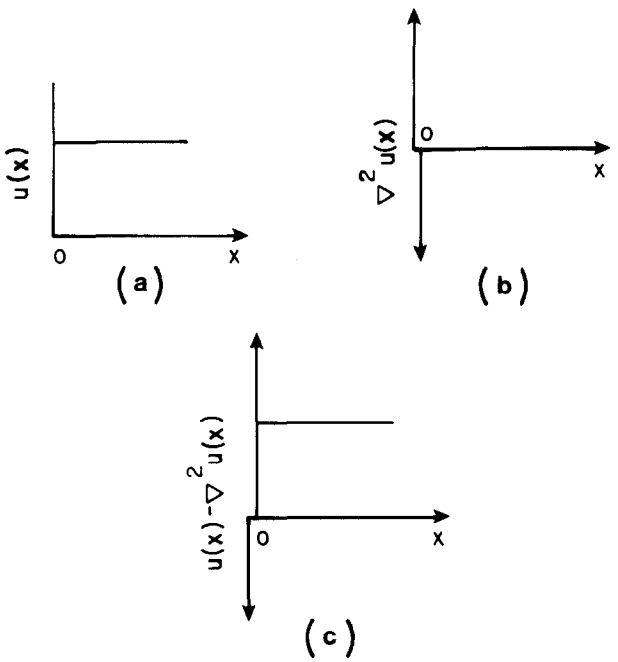

FIG. 6-1. (a) A step function $u(x)$; (b) the second derivative of $u(x)$, $\nabla^2 u(x)$; (c) $u(x) - \nabla^2 u(x)$.

operation can be formulated as

$$g'(x, y) = g(x, y) - \gamma \nabla^2 g(x, y) \tag{6-1}$$

where γ is a constant. Figure 6-1 illustrates a 1-dim. example of edge enhancement by an anti-diffusion operation on a smeared edge. Digital implementation of Eq. (6-1) is a matrix which has both positive and negative elements [9, 15, 57, 58]. This technique may yield a clear view of the edges; it may also enhance the noise.

Overemphasis on accidental fluctuations is one of the major problems with edge-enhancement techniques. A possible solution can be offered by edge enhancement along the direction of the local gradient [56]. This technique enhances the edge according to

$$g'(x, y) = g(x, y) - \gamma \frac{\delta^2 g(x, y)}{\delta n^2} \tag{6-2}$$

where

$$\frac{\delta^2 g(x, y)}{\delta n^2} = \frac{\dfrac{\delta^2 g}{\delta x^2}\left(\dfrac{\delta g}{\delta x}\right)^2 + 2\dfrac{\delta^2 g}{\delta x \delta y}\dfrac{\delta g}{\delta x}\dfrac{\delta g}{\delta x}\dfrac{\delta^2 g}{\delta y^2}\left(\dfrac{\delta g}{\delta y}\right)^2}{\left(\dfrac{\delta g}{\delta x}\right)^2 + \left(\dfrac{\delta g}{\delta y}\right)^2}.$$

It should be noted that the small scale curvature is probably due to noise. A modification of the above technique which enhances the contour along the gradient, and smooths the edge along the contour, has been proposed [62]. It is formulated as

follows:

$$g'(x, y) = g(x, y) - \gamma\left(\frac{\delta^2 g(x, y)}{\delta n^2} - \frac{1}{3}\frac{\delta g(x, y)}{\delta t^2}\right)$$

where

$$\frac{\delta^2 g(x, y)}{\delta t^2} = \frac{\frac{\delta^2 g}{\delta x^2}\left(\frac{\delta g}{\delta y}\right)^2 - 2\frac{\delta^2 g}{\delta x \delta y}\frac{\delta g}{\delta x}\frac{\delta g}{\delta y} + \frac{\delta^2 g}{\delta y^2}\left(\frac{\delta g}{\delta x}\right)^2}{\left(\frac{\delta g}{\delta x}\right)^2 + \left(\frac{\delta g}{\delta y}\right)^2} \tag{6-3}$$

which is the second-order derivative along the tangent of the contour. The computation is complicated. However, it does enhance the slope and suppress the accidental jaggedness.

A filtering technique using local statistics was first proposed by Wallis [63], and then extended by Lee [64, 65]. This technique tends to enhance subtle details. The algorithm is

$$g'(x, y) = \bar{g}(x, y) + k(g(x, y) - \bar{g}(x, y)) \tag{6-4}$$

where $\bar{g}(x, y)$ is the local gray level mean surrounding the pixel (x, y). It should be noted that in Eq. (6-4), if $k > 1$, the difference between the local mean and gray level at (x, y) is magnified, and the edge will be sharpened as if passed through a high-pass filter. When $k = 2$, Eq. (6-4) is equivalent to Eq. (6-1). If $0 < k < 1$, the difference is diminished, and the image will be smoothed as if acted upon by a low-pass filter. If $k = 0$, the operation is just a simple smoothing. Experiments [64] show that when k is large, all the fine details, including noise, are enhanced.

Another technique which emphasizes edges and cleans "salt and pepper" noise has been presented [43]. At the isolated noise pixels, the Laplacian $|\nabla^2 g(x, y)|$'s are very large. This technique performs an anti-diffusion operation as in Eq. (6-1) if $|\nabla^2 g(x, y)|$ is less than a prespecified threshold T. It smooths a pixel as Eq. (4-1) if $|\nabla^2 g(x, y)|$ is larger than the threshold. In other words,

$$g'(x, y) = \begin{cases} g(x, y) - \gamma\nabla^2 g(x, y) & \text{if } |\nabla^2 g(x, y)| \le T \\ \dfrac{1}{(2m+1)(2n+1)} \displaystyle\sum_{i=-m}^{m}\sum_{j=-n}^{m} g(x-i, y-j) & \text{if } |\nabla^2 g(x, y)| > T. \end{cases} \tag{6-5}$$

As shown in this equation, the enhancement technique requires the specification of γ and of threshold T; thus many trials are needed.

An anti-diffusion operation which takes advantage of electronic scanning has been suggested [66–69]. The basic idea is to simultaneously scan with two scanning spots, one fine and one coarse, and subtract the resulting images electronically. Let the fine

resolution image be $g(x, y)$, and the coarse resolution image be $\bar{g}(x, y)$. The algorithm of this technique can be described by Eq. (6-4).

7. FILTERING IN THE FREQUENCY DOMAIN

An image can be viewed as a matrix of points with each point represented by some gray level. It can also be considered as a combination of two-dimensional Fourier series with different frequencies. Thus, a picture can be represented uniquely in the frequency domain. Transformation from spatial domain to frequency domain can be achieved by the fast Fourier transform (FFT) algorithm [70–72].

It has been noticed [73] that low-frequency Fourier components correspond to a homogeneous object and background, and high frequencies are introduced by the occurrence of a sharp edge or noise. Thus, low-pass or high-pass filters can be employed to smooth the picture, or to enhance the sharp edges. The design of these filters has been well developed in digital signal processing [74, 75]. Figure 7.1 illustrates a block diagram of a filter in the frequency domain. The operation is global and context-free.

Duda and Hart [73] considered as a low-pass filter

$$H(f_x, f_y) = \left[(\cos \pi f_x)(\cos \pi f_y)\right]^{\alpha}, \quad \alpha > 1 \tag{7-1}$$

and as a high-pass filter

$$H(f_x, f_y) = 1 - \left[(\cos \pi f_x)(\cos \pi f_y)\right]^{\alpha} \quad \alpha \geq 1. \tag{7-2}$$

It has been shown that a low-pass filter removes the noise; however, it blurs the picture. High-pass filtering sharpens the edges, but it enhances the noise and roughens the object. A compromise filter, called a high-frequency-emphasis (HFE) filter, is proposed. This filter keeps the low frequency unchanged, and exaggerates the high frequency. Duda and Hart proposed the following HFE filter:

$$H(f_x, f_y) = 2.0 - \left[(\cos \pi f_x)(\cos \pi f_y)\right]^{\alpha} \quad \alpha \geq 1. \tag{7-3}$$

The Butterworth filter [74] with a cutoff frequency f_0 has been utilized by Gonzalez and Wintz [8]. Butterworth proposed a low-pass filter

$$H(f_x, f_y) = \frac{1}{1 + \left[\left(f_x^2 + f_x^2\right)^{1/2} / f_0\right]^{2n}}, \tag{7-4}$$

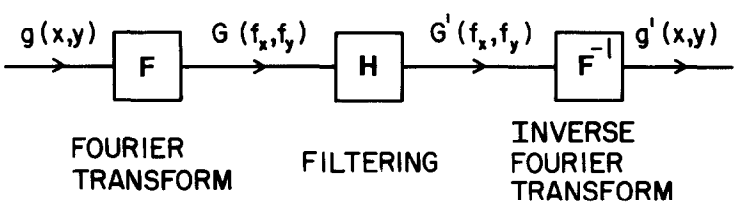

FIG. 7-1. A block diagram of filtering in the frequency domain.

a high-pass filter

$$H(f_x, f_y) = \frac{1}{1 + \left[f_0 / \left(f_x^2 + f_y^2 \right)^{1/2} \right]^{2n}}, \tag{7-5}$$

and a high-frequency-emphasis filter

$$H(f_x, f_y) = 1 + \frac{1}{1 + \left[f_0 / \left(f_x^2 + f_y^2 \right)^{1/2} \right]^{2n}}. \tag{7-6}$$

Hall *et al.* [39] applied an exponential filter to enhance radiographic images. Their exponential low-pass filter is given by

$$H(f_x, f_y) = \exp\left[-\left(f_x^2 + f_y^2 \right)^{1/2} / f_0 \right]^n, \tag{7-7}$$

their high-pass filter is represented by

$$H(f_x, f_y) = \exp\left[-f_0 / \left(f_x^2 + f_y^2 \right)^{1/2} \right]^n, \tag{7-8}$$

and their high-frequency-emphasis filter is

$$H(f_x, f_y) = 1 + \exp\left[-f_0 / \left(f_x^2 + f_y^2 \right)^{1/2} \right]^n. \tag{7-9}$$

Most of the energy of a picture is concentrated in the low-frequency portion. Hence, a logarithmic filter in the frequency domain is proposed [37]. Let

$$G(f_x, f_y) = |G(f_x, f_y)| e^{j\phi(f_x, f_y)} \tag{7-10}$$

which, after filtering, becomes

$$G'(f_x, f_y) = \left(\log |G(f_x, f_y)| \right) e^{j\phi(f_x, f_y)}. \tag{7-11}$$

Thus, the low-frequency portion is reduced more significantly than the high-frequency portion; high frequencies are emphasized more than low frequencies.

A similar filter, called α processing, has been suggested by Andrews [76]. The operation is

$$G'(f_x, f_y) = |G(f_x, f_y)|^{\alpha} e^{j\phi(f_x, f_y)}, \qquad 0 \le \alpha \le 2. \tag{7-12}$$

For small α, especially $\alpha = 0$, high-pass filtering results.

Another filter, call pruning [77], is designed to eliminate noise. This filter is a low-pass filter. By prespecifying a threshold T we obtain the filtered image as

$$G'(f_x, f_y) = \begin{cases} \left(|G(f_x, f_y)| - T \right) e^{j\phi(f_x, f_y)}, & \text{if } |G(f_x, f_y)| \ge T; \\ 0, & \text{if } |G(f_x, f_y)| < T. \end{cases} \tag{7-13}$$

Since the high frequency has less energy, the above filtering will remove the high-frequency portion.

Most of these techniques yield successful results. However, unless a special FFT processor is available, the computation is laborious and requires a huge storage. Note that these techniques require the specification of some constants, e.g., α, f_0; trial runs will make them even more time consuming.

Signal filtering has become a well-developed field [74, 75]. Many of its techniques can be expanded to process two-dimensional images. However, some of them are complex, and some require the specification of a cutoff frequency f_0 or threshold T.

8. CONCLUSIONS

In this paper, we survey existing image enhancement techniques. These techniques are classified into four categories: spatial smoothing, gray level rescaling, edge enhancement, and frequency-domain filtering. These procedures are reviewed according to their goals, limitations, practical applicability, and computational complexity. Most techniques are problem oriented. Therefore, we cannot provide general selection criteria. The reader must make his own choice on the basis of the problem at hand, his own judgment, and the available computational facilities.

ACKNOWLEDGMENTS

The authors express their appreciation for the secretarial assistance of Ms. Patricia Halaburka.

REFERENCES

1. K. Preston, Computer processing of biomedical images, *Computer* **9**, 1976, 54.
2. D. Ballard and J. Sklansky, Tumor detection in radiographs, *Comput. Biomed. Res.* **6**, 1973, 299.
3. D. E. Troxel and C. Lynn, Enhancement of news photos, *Computer Graphics Image Processing* **7**, 1978, 266.
4. E. C. Levinthal, W. B. Green, J. A. Cutts, E. D. Jahelka, R. A. Johansen, M. J. Sander, J. B. Seidman, A. T. Young, and L. A. Soderblom, Mariner 9—image processing and products, *Icarus* **18**, 1973, 75.
5. M. J. McDonnell, Restoration of Voyager I images of Io, *Computer Graphics Image Processing* **15**, 1981, 79.
6. D. C. C. Wang, A. H. Vagnucci, and C. C. Li, Image enhancement by gradient inverse weighted smoothing scheme, *Computer Graphics Image Processing* **15**, 1981, 167.
7. B. R. Hunt, The application of constrained least squares estimation to image restoration by digital computer, *IEEE Trans. Comput.* **C-22**, 1973, 805.
8. R. C. Gonzalea and P. Wintz, *Digital Image Processing*, (Applied Mathematics and Computation Series, no. 13), Addison–Wesley, Reading, Mass., 1977.
9. J. M. Prewitt, Object enhancement and extraction, in *Picture Processing and Psychopictorics*, (B. S. Lipkin and A. Rosenfeld, Eds.), p. 70, Academic Press, New York, 1970.
10. A. Rosenfeld and A. C. Kak, *Digital Picture Processing* (Computer Science and Applied Mathematics Series), Academic Press, New York, 1976.
11. H. C. Andrews, Digital image processing, *IEEE Spectrum*, April 1979, 38.
12. H. C. Andrews, Digital image restoration: A survey, *Computer* **7** (5), 1974, 36.
13. T. S. Huang, Some notes on film grain noise, in Woods Hole Summer Study Report on *Restoration of Atmospherically Degraded Images*, Vol. 2, Alexandria, Va., Defense Documentation Center, July 1966.
14. H. C. Andrews and B. R. Hunt, *Digital Image Restoration*, Prentice-Hall, New Jersey, 1977.
15. W. K. Pratt, *Digital Image Processing*, Wiley, New York, 1978.
16. J. C. Dainty and R. Shaw, *Image Science*, Academic Press, New York, 1974.
17. J. W. Goodman, Some fundamental properties of speckles, *J. Opt. Soc. Amer.* **66** (11) 1976, 1145.
18. A. Rosenfeld, *Picture Processing by Computer*, Academic Press, New York, 1969.

19. L. S. Davis, A. Rosenfeld, and J. Weszka, Region extraction by averaging and thresholding, *IEEE Trans. Syst. Man Cybern.* **SMC-5**, 1975, 383.
20. R. E. Graham, Snow removal—A noise-stripping process for picture signals, *IRE Trans. Inf. Theor.* **IT-8**, 1962, 129.
21. D. W. Brown, Digital computer analysis and display of the radionuclide scan, *J. Nucl. Med.* **7**, 1966, 740.
22. A. Lev, S. W. Zucker, and A. Rosenfeld, Iterative enhancement of noisy image, *IEEE Trans. Syst. Man Cybern.* **SMC-7**, 1977, 435.
23. M. Kuwahara, K. Hachimura, S. Eiho, and M. Kinoshita, Processing of RI-angiocardiographic images, in *Digital Processing of Biomedical Images*, (K. Preston and M. Onoe, Eds.), Plenum, New York, 1976.
24. F. Tomita and S. Tsuji, Extraction of multiple regions by smoothing in selected neighborhoods, *IEEE Trans. Syst. Man Cybern.* **SMC-7**, 1977, 107.
25. M. Nagao and T. Matsuyama, Edge preserving smoothing, *Computer Graphics Image Processing* **9**, 1979, 394.
26. G. L. Anderson and A. N. Netravali, Image restoration based on a subjective criterion, *IEEE Trans. Syst. Man Cybern.* **SMC-6**, 1976, 845.
27. J. G. Trussell, A fast algorithm for noise smoothing based on a subjective criterion, *IEEE Trans. Syst. Man Cybern.* **SMC-7**, 1977, 677.
28. J. W. Tukey, *Exploratory Data Analysis*, Addison–Wesley, Reading, Mass., 1977.
29. N. S. Jayant, Average and median-based smoothing techniques for improving digital speech quality in the presence of transmission errors, *IEEE Trans. Commun.* **COM-24**, 1976, 1043.
30. B. R. Frieden, A new restoring algorithm for the preferential enhancement of edge gradients, *J. Opt. Soc. Amer.* **66**, 1976, 280.
31. T. S. Huang, G. J. Yang, and G. Y. Tang, A fast two-dimensional median filtering algorithm, *IEEE Trans. Acoust. Speech Signal Process.* **ASSP-27**, 1979, 13.
32. P. Narendra, A separable median filter for image noise smoothing, *IEEE Trans. Pattern Anal. Mach. Intell.* **PAMI-3**, 1981, 20.
33. R. Kohler and H. Howell, Photographic image enhancement by superimposition of multiple images, *Photo. Sci. Eng.* **7**, 1963, 241.
34. R. Nathan, Picture enhancement for the moon, Mars and man, in *Pictorial Pattern Recognition*, (G. C. Cheng *et al.*, Eds.), p. 239, Thompson, Washington, D.C., 1968.
35. F. Billingley, Applications of digital image processing, *Appl. Opt.* **9**, 1970, 289.
36. E. Hall, Almost uniform distribution for computer image enhancement, *IEEE Trans. Comput.* **C-23**, 1974, 207.
37. H. C. Andrews, A. G. Tescher, and R. P. Kruger, Image processing by digital computer, *IEEE Spectrum* **9** (7) July 1972, 20.
38. E. B. Troy, E. S. Deutsch, and A. Rosenfeld, Gray-level manipulation experiments for texture analysis, *IEEE Trans. Syst. Man Cybern.* **SMC-3**, 1973, 91.
39. E. L. Hall, R. P. Kruger, S. J. Dwyer, D. L. Hall, R. W. McLaren, and G. S. Lodwick, A survey of preprocessing and feature extraction techniques for radiographic images, *IEEE Trans. Comput.* **C-20**, 1971, 103.
40. R. M. Haralick, K. Shanmugan, and I. Dinstein, Texture features for image classification, *IEEE Trans. Syst. Man Cybern.* **SMC-3**, 1973, 610.
41. D. J. Ketcham, R. W. Lowe, and J. W. Weber, Image enhancement techniques for cockpit display, TR-P74-530R, Display System Laboratory, Hughes Aircraft Co., Culver City, Calif., 1974.
42. R. Hummel, Histogram modification techniques, *Computer Graphics Image Processing* **4**, 1975, 209.
43. R. Hummel, Image enhancement by histogram transformation, *Computer Graphics Image Processing* **6**, 1977, 184.
44. W. Frei, Image enhancement by histogram hyperbolization, *Computer Graphics Image Processing* **6**, 1977, 286.
45. G. Wyszecki and W. S. Stiles, *Color Science*, Wiley, New York, 1967.
46. C. J. Bartleson and E. J. Breneman, Brightness perception in complex fields, *J.Opt. Soc. Amer.* 57, 1967, 953.
47. T. J. Stockham, Image processing in the context of a visual model, *Proc. IEEE* **60**, 1972, 828.
48. A. Rosenfeld and L. S. Davis, Iterative histogram modification, *IEEE Trans. Syst. Man Cybern.* **SMC-8**, 1978, 300.

49. S. Peleg, Iterative histogram modification, 2, *IEEE Trans. Syst. Man Cybern.* **SMC-8**, 1978, 555.
50. H. J. Zweig, E. B. Barrett, and P. C. Hu, Noise-cheating image enhancement, *J.Opt. Soc. Amer.* **65**, 1975, 1347.
51. F. Nadeni and A. A. Sawchuk, Detection of low-contrast image in film-grain noise, *Appl. Opt.* **17**, 1978, 2883.
52. E. E. Christensen, T. S. Curry, and J. Nunnally, *An Introduction to the Physics of Diagnostic Radiology*, Lee & Febiger, Philadelphia, 1972.
53. M. Mojab, L. Garcia, and G. Talge, A new subtraction technique using duplicating film as a final print, *Amer. J. Roentgenol.* **129**, 1977, 528.
54. R. A. Kruger, C. A. Mistretta, A. B. Crummy *et al.*, Digital *K*-Edge subtraction radiography, *Radiology* **125**, 1973, 243.
55. M. G. Ort, E. C. Gregg, and B. Kaufman, Subtraction radiography: Techniques and limitations, *Radiology* **124** (3), 1977, 65.
56. L. S. G. Kovasznay and H. M. Joseph, Image processing, *Proc. IRE* **43**, 1955, 560.
57. L. G. Roberts, Machine perception of three-dimensional solids, in *Optical and Electro-Optical Information Processing*, (J. T. Tippett *et al.*, Eds.), MIT Press, Cambridge, Mass., 1965.
58. A. Arcese, P. Mengert, and W. E. Trombini, Image detection through bipolar correction, *IEEE Trans. Inf. Theor.* **IT-16**, 1970, 534.
59. T. Nagai and T. A. Linuma, A comparison of differential and integral scans, *J. Nucl. Med.* **9**, 1968, 202.
60. A. Rosenfeld and J. Weszka, Picture recognition and scene analysis, *Computer* **9** (5), May 1976, 28.
61. I. E. Abdou and W. K. Pratt, Quantitative design and evaluation of enhancement/thresholding edge detectors, *Proc. IEEE* **67**, 1979, 753.
62. D. Gabor, Information theory in electron microscopy, *Lab. Invest.* **14**, 1965, 801.
63. R. H. Wallis, An approach for the space variant restoration and enhancement of images, *Proceedings, Symposium on Current Math. Prob. in Image Science*, Monterey, Calif., November 1976.
64. J. S. Lee, Digital image enhancement and noise filtering by use of local statistics, *IEEE Trans. Pattern Anal. Mach. Intell.* **PAMI-2**, 1980, 165.
65. J. S. Lee, Refined filtering of image noise using local statistics, *Computer Graphics Image Processing* **15**, 1981, 380.
66. S. W. Levine and H. Mate, Selected electronic techniques for image enhancement, Paper II in *Proceedings, Image Enhancement Seminar*, Soc. Photo. Instr. Engrs., Redondo Beach, Calif. 1963.
67. D. R. Craig, Disenhancement—A negative approach to a positive problem, Paper V in *Proceedings, Image Enhancement Seminar*, Soc. Photo. Instr. Engrs., Redondo Beach, Calif., 1963.
68. A. J. Hannum, Techniques for electronic image enhancement, Paper VII in *Proceedings, Image Enhancement Seminar*, Soc. Photo. Instr. Engrs., Redondo Beach, Calif., 1963.
69. W. F. Schreiber, Wirephoto quality improvement by unsharp masking, *Pattern Recog.* **2**, 1970, 171.
70. J. W. Cooley and T. W. Tukey, An algorithm for machine calculation of complex Fourier series, *Math. Comp.* **19**, 1965, 297.
71. R. C. Singleton, On computing the fast Fourier transform, *Commun. Assoc. Comput. Mach.* **10**, 1967, 647.
72. R. C. Singleton, An Algol procedure for the fast Fourier transform with arbitrary factors, Algorithm 339, *Commun. Assoc. Comput. Mach.* **11**, 1968, 776.
73. R. O. Duda and P. E. Hart, *Pattern Classification and Scene Analysis*, Wiley, New York, 1973.
74. A. V. Oppenheim and R. W. Schaefer, *Digital Signal Processing*, Prentice Hall, Englewood Cliffs, N. J., 1975.
75. T. S. Huang (Ed.), *Picture Processing and Digital Filtering*, Springer, New York, 1975.
76. H. C. Andrews, Monochrome digital image enhancement, *Appl. Opt.* **15**, 1976, 495.
77. P. P. Varoutas, L. R. Nardizzi, and E. M. Stokely, Digital image processing applied to scintillation images from biomedical systems, *IEEE Trans. Biomed. Eng.* **BME-24**, 1977, 337.
78. S. J. Riederer and R. A. Kruger, Intravenous digital subtraction: A summary of recent developments, *Radiology* **147**, 1983, 633.